Application of contrast-enhanced magnetic resonance imaging in the assessment of blood-cerebrospinal fluid barrier integrity

Verheggen, I.C.M.; Freeze, W.M.; Jong, J.J. de; Jansen, J.F.A.; Postma, A.A.; Boxtel, M.P. van; ... ; Backes, W.H.

Neuroscience and Biobehavioral Reviews 127 (2021) 171–183

Contents lists available at ScienceDirect

Neuroscience and Biobehavioral Reviews

journal homepage: www.elsevier.com/locate/neubiorev

Review article

Application of contrast-enhanced magnetic resonance imaging in the assessment of blood-cerebrospinal fluid barrier integrity

Inge C.M. Verheggen [a,b,*], Whitney M. Freeze [a,b,c], Joost J.A. de Jong [b,d], Jacobus F. A. Jansen [b,d], Alida A. Postma [b,d], Martin P.J. van Boxtel [a,b], Frans R.J. Verhey [a,b], Walter H. Backes [b,d,e]

[a] Alzheimer Center Limburg, Department of Psychiatry and Neuropsychology, Maastricht University, P.O. Box 616, 6200 MD Maastricht, the Netherlands
[b] School for Mental Health and Neuroscience (MHeNs), Maastricht University, P.O. Box 616, 6200 MD Maastricht, the Netherlands
[c] Department of Radiology, Leiden University Medical Center, Leiden, P.O. Box 9600, 2300 RC Leiden, the Netherlands
[d] Department of Radiology and Nuclear Medicine, Maastricht University Medical Center, P.O. Box 5800, 6202 AZ Maastricht, the Netherlands
[e] School for Cardiovascular Diseases (CARIM), Maastricht University, P.O. Box 616, 6200 MD Maastricht, the Netherlands

ARTICLE INFO

Keywords:
Blood-cerebrospinal fluid barrier
Choroid plexus
MRI
Contrast-enhanced
Aging

ABSTRACT

VERHEGGEN, I.C.M., W. Freeze, J. de Jong, J. Jansen, A. Postma, M. van Boxtel, F. Verhey and W. Backes. The application of contrast-enhanced MRI in the assessment of blood-cerebrospinal fluid barrier integrity.

Choroid plexus epithelial cells form a barrier that enables active, bidirectional exchange between the blood plasma and cerebrospinal fluid (CSF), known as the blood-CSF barrier (BCSFB). Through its involvement in CSF composition, the BCSFB maintains homeostasis in the central nervous system. While the relation between blood-brain barrier disruption, aging and neurodegeneration is extensively studied using contrast-enhanced MRI, applying this technique to investigate BCSFB disruption in age-related neurodegeneration has received little attention. This review provides an overview of the current status of contrast-enhanced MRI to assess BCSFB permeability. Post-contrast ventricular gadolinium enhancement has been used to indicate BCSFB permeability. Moreover, new techniques highly sensitive to low gadolinium concentrations in the CSF, for instance heavily T2-weighted imaging with cerebrospinal fluid suppression, seem promising. Also, attempts are made at using other contrast agents, such as manganese ions or very small superparamagnetic iron oxide particles, that seem to be cleared from the brain at the choroid plexus. Advancing and applying new developments such as these could progress the assessment of BCSFB integrity.

1. Introduction

Over the last years, there has been great interest in studies investigating the association between blood-brain barrier (BBB) disruption, aging and neurodegeneration (Erdő et al., 2017; van de Haar et al., 2016; Montagne et al., 2017; Zlokovic, 2008). The most important function of the BBB involves maintaining homeostasis in the central nervous system (CNS) by the regulated exchange of valuable biomolecules, blocking the entrance of pathogens and clearing waste products from the internal milieu. This function is actually shared by the choroid plexus epithelial cells, that control the exchange between the blood and the cerebrospinal fluid (CSF), and thereby form the blood-CSF

Abbreviations: 3D-real IR, three-dimensional-real inversion recovery; Aβ, Amyloid-β protein; AD, Alzheimer's disease; AGES, Advanced glycation end products; ASL, Arterial spin labelling; BBB, Blood-brain barrier; BCSFB, Blood-cerebrospinal fluid barrier; BDNF, brain-derived neurotrophic factor; CCLL11, C-C motif chemokine; CNS, Central nervous system; CSF, Cerebrospinal fluid; CVOs, Circumventricular organs; DCE, Dynamic-contrast enhanced; DSC, Dynamic susceptibility-contrast; FLAIR, Fluid-attenuated inversion-recovery; GBCA, Gadolinium-based contrast agent; GDNF, Glial-cell derived neurotrophic factor; hT2w-FLAIR, Heavily T2-weighted fluid-attenuated inversion recovery; IL-4, Interleukin-4; iNPH, Idiopathic normal pressure hydrocephalus; ISF, Interstitial fluid; LRP-1/2, Lipoprotein receptor-related protein 1/2; MCAO, Middle cerebral artery occlusion; MEMRI, Manganese-enhanced MRI; MMP, Matrix metalloproteinases; MPDZ, Multiple PDZ-domain; MS, Multipele sclerosis; NGF, Nerve growth factor; NMOSD, Neuromyelitis optica spectrum disorder; RAGE, Receptors for advanced glycation end products; Th2, T-helper type 2; TTR, Transthyretin; VSOPS, Very small superparamagnetic iron oxide particles; eu-VSOPS, europium-doped VSOPs.

* Corresponding author at: Alzheimer Center Limburg, Department of Psychiatry and Neuropsychology, Maastricht University, P.O. Box 616, 6200 MD Maastricht, the Netherlands.
E-mail address: inge.verheggen@maastrichtuniversity.nl (I.C.M. Verheggen).

https://doi.org/10.1016/j.neubiorev.2021.04.025
Received 16 December 2020; Received in revised form 15 April 2021; Accepted 22 April 2021
Available online 27 April 2021

barrier (BCSFB) (Johanson, 2017). The finding that age-associated damage to the barriers can disrupt balance in the internal milieu and contribute to the neurodegenerative cascade, applies to both the BBB and BCSFB. The role of the BCSFB in the production of CSF has been appreciated for a long time, while its function in maintaining homeostasis in the CNS has often been overlooked (Ghersi-Egea and Strazielle, 2001). Investigating BCSFB disruption, and its possible connection to aging and neurodegeneration, could shed more light on age-related decline.

Broadening the focus from only the BBB to also investigating BCSFB disruption raises the question of what methods can be used to accurately measure BCSFB permeability. For BBB disruption, measuring the spread of a contrast agent from the vasculature to the brain with MRI has produced new insights, for instance the detection of subtle BBB leakage in neurodegenerative disorders (Starr et al., 2009). Therefore, it would be interesting to investigate whether contrast enhancement on MRI could also be used to obtain information on BCSFB permeability, and if so, how this technique should be implemented. To address these points, we conducted a literature review to obtain an overview of what has already been investigated on BCSFB permeability using contrast-enhanced MRI in both animal and human studies. From this overview, we attempted to outline what techniques hold most promise for the future of assessing BCSFB integrity.

1.1. Normal function of the BCSFB

The BCSFB is formed by choroid plexus epithelial cells. The choroid plexus is located at the inner ventricular surface of the lateral ventricles and at the roof of the third and fourth ventricle (Fig. 1A) (Liddelow, 2015; Wolburg and Paulus, 2010). The blood vessels in the choroid plexus are fenestrated, and choroid plexus epithelial cells connected by tight junctions surround the fenestrated capillaries to form a barrier for the molecules that leak from these capillaries (Fig. 1B) (Johanson, 2017; Balusu et al., 2016).

The choroid plexus is considered the most important structure in the production of CSF (Khasawneh et al., 2018). Driven by the pressure gradient between blood and ventricles, blood plasma is filtered by the choroid plexus fenestrated capillaries and then transported across the

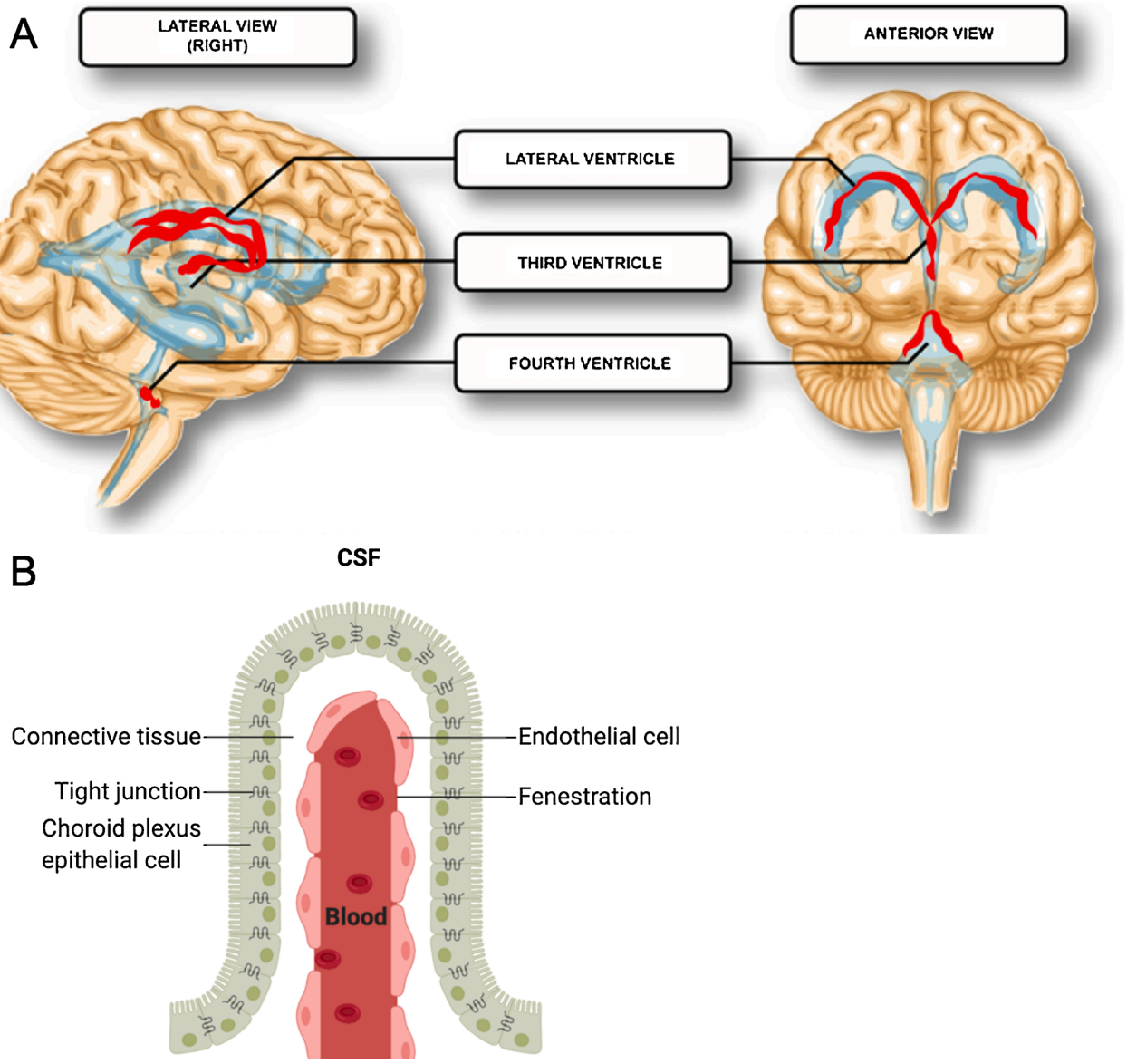

Fig. 1. The choroid plexus. A: The location of the choroid plexus (red ribbons) in the lateral ventricles, and third and fourth ventricle. Figure obtained from (Liddelow, 2015), under the Creative Commons Attribution 4.0 License (CC BY 4.0). B: Schematic overview on the cellular level of the choroid plexus forming the blood-CSF barrier. Figure created with BioRender.com.

choroid plexus epithelial cells to become part of the CSF (Brinker et al., 2014). An alternative theory opposes the classical view that CSF production is located in a single organ, and instead states that the CSF is produced and absorbed throughout the whole circulatory system at the perivascular spaces (Orešković and Klarica, 2010, 2014). However, this theory does not account for the ebbs and flows of CSF or the net flow (Khasawneh et al., 2018; Spector et al., 2015a), and needs independent confirmation. Moreover, a number of reviews have since refuted this theory in favour of evidence of secretion by the choroid plexus (Bateman and Brown, 2012; Hladky and Barrand, 2014; Spector et al., 2015b), which is more generally accepted. Therefore, in this review, we will focus on fluid exchange at the level of the choroid plexus.

Besides functioning as a barrier, the choroid plexus epithelial cells enable active, bidirectional exchange between the blood and CSF (Johanson, 2017). CSF has a different composition than blood plasma. The concentrations of Cl^- and Mg^{2+} ions are higher in the CSF, and the concentrations of Na^+, K^+ and Ca^{2+} ions are lower in the CSF compared to the blood plasma (Davson and Segal, 1996). Moreover, the concentrations of glucose and amino acids in the CSF are approximately half of that in the blood plasma. These differences indicate that CSF is not just the result of blood plasma filtration by the choroid plexus (Segal, 2000).

The BCSFB contains several transporters involved in the clearance of the neurotoxic amyloid-β protein (Aβ), known for its role in the pathogenesis of Alzheimer's disease (AD), such as lipoprotein receptor-related protein 1 and 2 (LRP-1 and LRP-2), receptors for advanced glycation end products (RAGE) and p-glycoprotein (p-gp). The BCSFB also secretes the protein transthyretin (TTR), which, just like the transporters, binds soluble Aβ to facilitate its clearance from the brain, and prevents the formation of Aβ plaques (Balusu et al., 2016; Serot et al., 1997).

Other BCSFB transporters supply nutrients and neurotrophic factors to the CSF, and the CSF facilitates their distribution over the whole CNS. Neurotrophic factors are produced at the BCSFB, such as glial cell-derived neurotrophic factor (GDNF), brain-derived neurotrophic factor (BDNF) and nerve growth factor (NGF) (Borlongan et al., 2004). Moreover, the BCSFB plays a role in the immune response, as the choroid plexus epithelial cells can trigger an inflammatory response by the production of chemokines and cytokines, and also as T-lymphocytes can enter the brain through the BCSFB (Balusu et al., 2016).

1.2. The blood-cerebrospinal fluid barrier in aging and neurodegeneration

The BCSFB undergoes structural and functional changes during normal aging (Balusu et al., 2016). The structural changes involve atrophy of the choroid plexus epithelial cells, evident by a decrease in height and thickening of the basement membrane (Serot et al., 2001a). Also, neurotoxic proteins accumulate in the choroid plexus epithelial cells (Balusu et al., 2016; Serot et al., 2003), such as Biondi bodies and lipofuscin deposits, that alter cell function (Wen et al., 1999). A possible functional change is a decrease in CSF secretion, that has been well established in animal studies (Preston, 1999; Wilson et al., 1999; Chen et al., 2009). However, in human studies, the results are less clear. One study found that the elderly had significantly lower CSF production compared to the young (May et al., 1990), but this study used a modified Masserman method, which has been criticized as being unusable with different CSF volumes (Fishman, 2002). Moreover, another study did not find a significant difference in CSF production between an older and a younger group (Gideon et al., 1994). CSF volume increases during aging due to cerebral atrophy (Tanna et al., 1991), which could lead to decreased CSF turnover, especially when combined with decreased CSF production (Serot et al., 2003).

The structural and functional changes in the BCSFB during normal aging are exacerbated in AD (Balusu et al., 2016; Serot et al., 2003). Choroid plexus epithelial cells, for instance, show more shrinkage and increased thickening of the basement membrane (Serot et al., 2000). Also, a stronger decrease in CSF production has been found in AD (Silverberg et al., 2001, 2003), but again the Masserman Technique has been used, which could give unreliable results with different CSF volumes (Fishman, 2002). However, a large increase in CSF volume in AD (De Leon et al., 2004), could still lead to a large decrease in CSF turnover, which promotes the glycation of proteins and increases the amount of advanced glycation end products (AGEs), that are prone to aggregation and trigger age-related pathology (Vitek et al., 1994).

The increase of amyloid protein oligomers in the brain is due to increased production and decreased clearance of Aβ, combined with decreased CSF turnover and increased protein glycation (Serot et al., 2003; Chen et al., 2017). The BCSFB contains transporters to take up Aβ for degradation, but AD impairs the choroid plexus epithelial cell lysosomal function (Balusu et al., 2016). Rather than being cleared, Aβ accumulates in the choroid plexus epithelial cells, which can lead to oxidative stress and cell death and increase BCSFB disruption (Vargas et al., 2010). Moreover, the BCSFB transporters that normally clear Aβ from the CSF to the blood are compromised in AD, which can lead to extracellular Aβ accumulation at the apical membrane, which can then further increase BCSFB disruption (Vargas et al., 2010; Mesquita et al., 2012). This can impair the ability of the BCSFB to secrete Aβ-binding proteins, that normally interact with Aβ to facilitate its clearance (Mesquita et al., 2012; Crossgrove et al., 2005). One of these proteins is for instance TTR, which is synthesized and secreted by the choroid plexus, and normally binds and stabilizes soluble Aβ to facilitate its clearance and prevent the formation of Aβ plaques (Li et al., 2000; Tang et al., 2004). A decrease in TTR level, which has been found in AD, can therefore lead to more Aβ accumulation in the brain (Serot et al., 1997; Chen et al., 2005).

Transport of folate and vitamin B12 from the blood to the CSF through the choroid plexus is also decreased in AD (Ikeda et al., 1990; Serot et al., 2001b). Folate and vitamin B12 catalyze methylation, which means adding a methyl group to a substrate, and this process is for instance important for the formation of neurotransmitters, myelin and the regulation of Aβ levels (Selhub et al., 2010). Lower levels in the CSF, in combination with a decrease in CSF turnover, can lead to less folate and vitamin B12 being distributed over and supplied to the brain (Serot et al., 2003). Decreased expression of tight junctions on the choroid plexus epithelial cells has also been found in AD (Bergen et al., 2015). These changes are associated with increased epithelial leakage, which can in turn affect CNS homeostasis and aggravate neurodegenerative processes.

1.3. The immune response in the choroid plexus during aging

Immune cell trafficking into the CNS increases with age (Baruch et al., 2015). An important component of the immune response are T-lymphocytes recognizing antigens in the CNS, which is important to maintain the integrity of the CNS, and support neurogenesis, neurotrophic factor production, and hippocampus-dependent learning and memory (Ziv et al., 2006; Moalem et al., 1999). T-lymphocytes accumulate at the choroid plexus (Engelhardt and Ransohoff, 2005). As the choroid plexus is involved in the communication between the blood and CSF, T-lymphocytes at the choroid plexus can react to antigens in the CSF, and subsequently release cytokines that influence the choroid plexus epithelial cells and the CNS (Emerich et al., 2005). The choroid plexus was demonstrated to contain CNS-specific $CD4^+$ memory cells, which contain receptors for T-lymphocytes that specifically react to antigens in the CNS, and mainly secrete the cytokine interleukin-4 (IL-4), which is involved in neuroprotection (Baruch et al., 2013).

During aging, T-lymphocytes in the choroid plexus maintain their CNS specificity, but the response shifts towards the T-helper type 2 (Th2) cells (Baruch et al., 2013). The Th2 response increases the amount of IL-4 that is released into the CSF (Shearer, 1997). However, overexpression of IL-4 actually has a detrimental effect on CNS homeostasis, and consequently, brain functioning. Low levels of IL-4 would normally induce BDNF production, which is beneficial for CNS homeostasis, while high levels of IL-4 lead to BDNF dysregulation. Also, high levels of IL-4

induce the production of C-C motif chemokine 11 (CCL11) which suppresses IL-4 and interferes with IL-4 signaling (Stevenson et al., 2009). It has been demonstrated that the immune response mediated by T-lymphocytes is important for hippocampus-related cognitive functions (Ziv et al., 2006; Kesslak et al., 1998), and it was suggested that dysregulation of T-lymphocyte signaling at the choroid plexus epithelial cells could be a cause of age-related cognitive decline (Baruch et al., 2013).

1.4. The relevance of the development of imaging techniques for the central nervous system barriers

Homeostasis in the CNS is dependent on the dynamics between the neurofluids, a collective name for all fluids inside the CNS, namely the blood, CSF and ISF (Agarwal et al., 2019). Several diseases have been associated with a disturbance in neurofluid dynamics, such as sleep disorders (DiNuzzo and Nedergaard, 2017), AD (Schubert et al., 2019), Parkinson's disease (Sundaram et al., 2019), traumatic brain injury (Christensen et al., 2020) and stroke (Gaberel et al., 2014). A disturbance in neurofluid dynamics can be caused by BBB disruption, BCSFB disruption and/or glymphatic dysfunction. The glymphatic system is a waste clearance system using the microcirculation of the CSF. Some publications report that CSF is exchanged with ISF due to convective flow from the para-arterial to the paravenous spaces, to clear solutes from the interstitial space (Iliff et al., 2012; Kress et al., 2014). Recently, however, other researchers claim that the evidence for convective flow in the brain parenchyma is lacking (Smith and Verkman, 2019; Abbott et al., 2018). It has been proposed that convective flow in the para-arterial spaces allows CSF to enter the brain parenchyma, but CSF moves through the interstitial space and exchanges with ISF through diffusion rather than convective flow (Abbott et al., 2018). Diseases in which BBB disruption, BCSFB disruption and/or glymphatic dysfunction, and thus disturbance in neurofluid dynamics, are involved can be grouped under the term CNS interstitial fluidopathies (Taoka and Naganawa, 2020). The development of dedicated imaging techniques to obtain specific information on the dynamics between neurofluids may help in understanding the underlying pathophysiology of CNS interstitial fluidopathies, and might even help in the development of novel common treatment options.

1.5. Assessing barrier permeability

Studies into BCSFB disruption mostly use the CSF/serum albumin ratio as an index of BCSFB integrity, in which the level of the blood-specific protein albumin is measured in the CSF by lumbar puncture and in the serum by venipuncture (Ott et al., 2018; Chalbot et al., 2011; Goldim et al., 2019; Okamura et al., 2010). For the in vivo assessment of BBB disruption, however, an increasingly used method is dynamic contrast-enhanced (DCE) MRI, in which a gadolinium-based contrast agent (GBCA) is intravenously injected during scanning. The transfer of the contrast from the blood plasma into the brain tissue is measured over time, after which pharmacokinetic modelling is used to separate the blood component from the tissue component and calculate the leakage rate (Raja et al., 2018). Unlike the CSF/serum albumin ratio, DCE MRI can measure very subtle leakage in a specific brain region, and can therefore separate BBB disruption from BCSFB disruption (van de Haar et al., 2014).

The detection of contrast enhancement on MRI to calculate BBB leakage has produced interesting results and provided new insights into the role of BBB disruption in aging and neurodegeneration (van de Haar et al., 2014; Verheggen et al., 2020a). This approach may also be useful for calculating BCSFB leakage, but this has been given less attention. Therefore, this paper explores how contrast enhancement on MRI can be used to assess BCSFB permeability. For this purpose, we conducted a literature review to make an inventory of methods using contrast enhancement on MRI for BCSFB permeability assessment, and to summarize the findings of the available studies.

2. Methods

To explore how contrast enhancement on MRI is being used to assess BCSFB permeability, a literature search was conducted in the PubMed database. The search terms *blood-cerebrospinal fluid barrier* (using MeSH terminology and the synonyms *blood-cerebrospinal fluid, blood-CSF barrier, blood-CSF, BCSFB, BCB,* or *choroid plexus*), *contrast agent* (using MeSH terminology and the synonyms *contrast, contrast-enhanced,* or *gadolinium*) and *MRI* (using MeSH terminology and the synonyms *magnetic resonance imaging, imaging,* or *MR imaging*) were used. Papers from the years 2000 up to and including 2020 written in English were included in the search. The search produced in total 254 results.

All 254 papers were screened using the title and abstract to check whether they actually applied contrast-enhanced MRI to assess BCSFB function. Papers were included when they met the following inclusion criteria: 1) reporting an original study. 2) combining MRI with administration of some type of contrast agent. 3) Investigating BCSFB permeability by assessing contrast enhancement dynamics at the choroid plexus and/or ventricular system.

After this screening, 20 papers remained. These papers were fully read and cross-referencing was used. From each study, we extracted the following information: sample, age of participants in human studies, MRI technique, contrast agent type and dosage, injection method, imaging delay time after contrast injection and indicator of BCSFB permeability. In the sections below, we describe the main findings of each study to give a complete summary of what has already been done and what can already be concluded regarding the use of contrast enhancement on MRI to assess BCSFB permeability.

3. Results

3.1. Animal studies

See Table 1 for a summary of the included animal studies.

3.1.1. Gadolinium enhancement in the ventricles

Nixon et al. (2008) used post-contrast T1-weighted MRI immediately after intravenous administration of a GBCA and assessed the hyperintense volume in the ventricles. Hyperintense areas were manually defined and the intensities of those pixels summed. The authors demonstrated that the GBCA was evenly distributed throughout the ventricles of healthy rats given ethanol and thiamine-depleted rats given glucose (Nixon et al., 2008). They conclude that GBCA must have entered the ventricles through the choroid plexus, and impairment in the choroid plexus seems to be an early event in ethanol intoxication and alcoholism.

Batra et al. (2010) used fluid-attenuated inversion recovery (FLAIR) before and 10 min after intravenous administration of a GBCA in rats that underwent unilateral middle cerebral artery occlusion (MCAO) or sham surgery. Contrast injection and imaging were performed 1 h, 24 h or 48 h after reperfusion. BCSFB permeability was measured using the change in signal intensity in the ventricles from the pre-contrast to post-contrast images, with normalization by pre-contrast values. Change in signal intensity in the ventricles of the MCAO rats was compared to the intensity change in the sham rats. The 1 -h, 24 -h and 48 -h groups had significantly more gadolinium enhancement than the sham group. The authors also investigated whether the matrix metalloproteinases 2 and 9 (MMP-2 and MMP-9), which are often found after a stroke (Montaner et al., 2001), are associated with BBB and BCSFB disruption (Batra et al., 2010). Plasma MMP-9 levels were indeed significantly correlated with gadolinium enhancement in the ventricles in the 1 -h group, so plasma MMP-9 could be indicative of acute BCSFB disruption. The authors emphasize the research opportunities of early BCSFB disruption, and the possibility of combining imaging markers such as post-contrast FLAIR gadolinium enhancement with blood biomarkers.

Saito et al. (2011) investigated whether changes in BBB and BCSFB

Table 1
Overview of included animal studies.

Study	Sample	MRI technique	Contrast agent type and dosage	Injection method	Imaging delay time after contrast injection	Indicator of BCSFB permeability
Nixon et al. (2008)	141 healthy, female rats	Post-contrast T1-weighted	100 µl of 20 % solution Gd-DTPA	Intravenous	Immediately after	Hyperintense volume in the ventricles
Batra et al. (2010)	Male, spontaneously hypertensive rats 6 naive 6 sham surgery 6 MCAO, 1 h since reperfusion 6 MCAO, 24 h since reperfusion 6 MCAO, 48 h since reperfusion	Pre- and post-contrast FLAIR	0.2 ml Gd-DTPA	Intravenous	10 min	Gadolinium enhancement ratio of the ventricles: change in intensity from the pre-contrast to post-contrast, with normalization by pre-contrast values
Saito et al. (2011)	20 neonatal, male rats	Pre- and post-contrast T1-weighted	0.004 ml/g Gd-DTPA	Intravenous	During	Gadolinium enhancement ratio of the ventricles: intensity after contrast divided by intensity before contrast
Ichikawa et al. (2011)	45 male rats with induced meningitis	Pre- and post-contrast T1-weigthed	0.2 mmol/kg Gd-DTPA	Intravenous	5 min	Gadolinium enhancement ratio of the lateral ventricles: change in intensity due to contrast compared to the native signal
Yang et al. (2019)	112 mice with 10 MPDZ knockout	Post-contrast T1-weighted	0.1 mmol/kg Gd-DTPA	Intravenous	Immediately after	Gadolinium enhancement ratio of the ventricles: total intensity divided by the difference between maximum and minimum intensity
Jost et al. (2016)	18 healthy, male rats	Pre- and post-contrast hT2w-FLAIR	5 GBCA groups 1 mmol Gd/kg	Intravenous	1 min	Qualitative evaluation of intensity increase in the CSF spaces
Jost et al. (2017)	48 healthy, male rats	Pre- and post-contrast hT2w-FLAIR	7 GBCA groups 1.8 mmol Gd/kg	Intravenous	9 and 24 min and 4 h	Gadolinium enhancement ratio of the CSF cavities: change in intensity from pre-contrast to post-contrast
Nathoo et al. (2016)	Male rats 2 cold injury model 5 LPS treated 7 hypoxia	Pre- and post-contrast T1-weighted	0.5 mmol/kg gadodiamide	Intravenous	Immediately after	Average intensity in the ventricles and periventricular structures of a series of pre-contrast images and a series of post-contrast images
Aoki et al. (2004)	28 male, healthy rats	Pre- and post-contrast T1-weighted	884.3 µmol/kg $MnCl_2$	Intravenous	0–2 hours, 1 day, 2 or 4 days or 2 weeks	Change in intensity from the pre-contrast to post-contrast images in the choroid plexus, ventricles and CVOs
Millward et al. (2013)	16 female mice from a MS mouse model	Pre- and post-contrast T2*-weighted	0.2 mmol/kg VSOPs	Intravenous	24 h	Presence of hypointense lesions in the choroid plexus compared to pre-contrast
Millward et al. (2019)	18 female mice from a MS mouse model	Pre- and post-contrast T2*-weighted	0.2 mmol/kg eu-VSOPs	Intravenous	24 h	Presence of hypointense lesions in the choroid plexus compared to pre-contrast

Abbreviations: Gd-DTPA = gadopentetate dimeglumine (gadolinium- diethylenetriamine pentaacetic acid); FLAIR = fluid-attenuated inversion recovery; MCAO = middle cerebral artery occlusion; MPDZ = gene for the multiple PDZ-domain protein; GBCA = gadolinium-based contrast agent; hT2w-FLAIR = heavily T2-weighted FLAIR; LPS = lipopolysaccharide (causing inflammation); $MnCl_2$ = manganese chloride; CVOs = circumventricular organs; MS = multiple sclerosis; VSOPs = very small superparamagnetic iron oxide particles.

integrity in prenatally irradiated rats could be detected using pre- and post-contrast T1-weighted MRI with intravenous administration of a GBCA and perfusion MRI (Saito et al., 2011). Signal intensity after GBCA administration was divided by signal intensity before GBCA administration to obtain the gadolinium enhancement ratio. No significant enhancement ratio was found in the ventricles after administration of GBCA, but perfusion MRI did demonstrate decreased cerebral blood flow, which the authors attributed to abnormal capillaries and arteries. These results were explained as the prenatally irradiated rats having a normally formed BBB and BCSFB, but immature capillary development.

Ichikawa et al. (2011) used T1-weighted MRI before and 5 min after intravenous administration of a GBCA, to investigate early changes in CNS barrier permeability in rats with induced meningitis (Ichikawa and Itoh, 2011). The gadolinium enhancement ratio was calculated by the change in signal intensity due to the GBCA relative to the native signal intensity (Ichikawa et al., 2010). However, while meningitis is associated with BBB disruption (Pfister et al., 1994), the authors did not observe a significant gadolinium enhancement ratio in the lateral ventricles indicative of BCSFB disruption. A significant enhancement ratio was found in the subarachnoid space, indicating that GBCAs could cross the arachnoid membrane (Ichikawa and Itoh, 2011).

Yang et al. (2019) investigated whether the multiple PDZ-domain (MPDZ) gene is important for the integrity of the BCSFB (Yang et al., 2019). The MPDZ protein is located close to the tight junctions of the choroid plexus epithelial cells and mutations in the MPDZ gene have been associated with hydrocephalus, which involves impairment in CSF circulation and causes CSF to accumulate in the ventricles (Feldner et al., 2017). The authors used T1-weighted MRI immediately after intravenous administration of a GBCA (Yang et al., 2019) in normal mice and MPDZ-knockout mice (Milner et al., 2015). The gadolinium enhancement ratio was calculated as the total intensity divided by the difference between the maximum and minimum intensity. Only in the MPDZ-knockout mice, significant gadolinium enhancement was found in the ventricles, and this GBCA leakage was attributed to choroid plexus epithelial cell deficits, demonstrating that the MPDZ gene is indeed important for choroid plexus integrity and function.

3.1.2. *New techniques*

Jost et al. (2016) used gadolinium enhancement to investigate how substances can infiltrate the CSF in healthy rats, so in the absence of a disorder or genetic deficit impairing BCSFB integrity. Therefore, a more sensitive method to measure more subtle leakage was needed (Jost et al.,

2016). Heavily T2-weighted fluid-attenuated inversion recovery (hT2w-FLAIR) was applied before and 1 min after intravenous administration of a GBCA, as this technique is especially sensitive to detect low concentrations of GBCA within the CSF (Naganawa et al., 2010; Freeze et al., 2019). The authors compared intravenous administration of three linear and two macrocyclic GBCAs (Jost et al., 2016). On T1-weighted images, no gadolinium enhancement could be detected, but with hT2w-FLAIR, qualitative evaluation demonstrated that signal intensity in the CSF spaces (arachnoid space, cerebral aqueduct and inner auditory canal) increased after GBCA administration for each type of GBCA.

Jost et al. (2016) noted that they may not have included the time point of maximal enhancement, and could not determine the precise location of infiltration from GBCAs into the brain (Jost et al., 2016). Therefore, in a subsequent study, Jost et al. (2017) elaborated on their previous study by investigating whether the blood-CSF pathway could be an alternative route for GBCAs to enter the brain (Jost et al., 2017). HT2w-FLAIR MRI was performed in healthy rats before and 1 min after intravenous administration, with temporal evaluations at 9 and 25 min after administration, and again 4 h after administration. Signal intensity in the CSF cavities (third and fourth ventricles, subarachnoid space and cerebral aqueduct) increased significantly from pre-contrast to post-contrast images. Signal intensity increased at the fastest rate in the ventricles and cerebral aqueduct, which supports the idea that GBCAs enter the CNS through the choroid plexus.

By modelling the time course of the spread of a GBCA with DCE MRI, BBB leakage in a single voxel can potentially be calculated, but this requires modelling assumptions (Roberts and Mikulis, 2007). Nathoo et al. (2016) developed a novel, voxel-based analysis technique to visualize BBB leakage at the level of a single voxel, that does not require any modelling assumption (Nathoo et al., 2016). With this technique, the average signal intensity of a series of pre-contrast T1-weighted images before intravenous administration of a GBCA and a series of post-contrast T1-weighted images was calculated, and statistically compared. This technique would prevent selection of an arbitrary ROI, which could be beneficial for investigating processes such as hypoxia that lead to nonspecific and diffuse BBB disruption (Natah et al., 2009). Though the aim was to assess BBB disruption, the application of this technique in rats with induced cortical injury, hypoxia or lipopolysaccharide-associated inflammation, demonstrated major BCSFB disruption in hypoxia and inflammation, with increased GBCA transfer into the ventricles and periventricular enhancement (Nathoo et al., 2016).

3.1.3. Other contrast agents

In MRI studies, gadolinium compounds are most frequently used as contrast agent, but other contrast agents are available. Manganese ions, for instance, demonstrate T1-shortening in tissues and appear hyperintense on post-contrast T1-weighted images (Wesolowski and Kaiser, 2016). While gadolinium has a short window of enhancement, manganese enhancement persists beyond this window. Post-contrast manganese-enhanced imaging always takes place at least 30 min after contrast administration. Aoki et al. (2004) used T1-weighted MRI before and at various time intervals after intravenous administration of a manganese chloride solution in healthy rats (Aoki et al., 2004). The authors demonstrated increased signal intensity compared to the pre-contrast images in the choroid plexus 10 min after administration, followed by the ventricles and circumventricular organs (CVOs).

In the field of experimental biomedical imaging, attempts are being made to discover new contrast agents that have relevant T1 and T2 contrast properties and can be detected by both MRI and optical imaging. Millward et al. (2013) tried to detect inflammatory lesions at the BCSFB at an early stage in a mouse model of multiple sclerosis (Millward et al., 2013). Intravenous administration of very small superparamagnetic iron oxide particles (VSOPs) was used, as these particles can be phagocytosed (Stroh et al., 2006) and efficiently extravasated, and highlight barrier disruptions (Wuerfel et al., 2007). VSOPs accumulated in the choroid plexus of mice with T-cell transfer, but without clinical signs of overt inflammation, although this accumulation could only be detected with histology, and not with MRI (Millward et al., 2013). This accumulation could not be explained by normal diffusion, as it was absent in mice without T-cell transfer. These results indicate that the choroid plexus may be a site for early pathological changes in the immune response of the CNS. At peak disease, VSOP accumulation in the choroid plexus could be detected as hypointense lesions visible on T2*-weighted images 24 h after intravenous administration, that were not present on pre-contrast images. In a later study, Millward et al. (2019) used europium-doped VSOPs (eu-VSOPs), which have fluorescent properties and can also be detected with fluorescence microscopy (Millward et al., 2019; Kobayashi et al., 2017). 24 h after intravenous administration, T2*-weighted imaging demonstrated eu-VSOPS accumulation in the choroid plexus in the mouse model of multiple sclerosis. Moreover, the hypointense lesions indicating eu-VSOP accumulation were absent during the remission phase, while mice did show eu-VSOPs enhancement during relapse.

3.2. Human studies

See Table 2 for a summary of the included human studies.

Hsu et al. (2005) reported on two cases (a child with craniosynostosis and hydrocephalus and a man with focal seizure) showing diffuse CSF enhancement on post-contrast T1-weighted MRI immediately after intravenous administration of a GBCA compared with the pre-contrast T1-weighted images (Hsu and Chen, 2005). The authors considered CSF enhancement to be a rare phenomenon that implies BCSFB breakdown, but speculated that, due to developments such as imaging with a longer delay after contrast administration (KNUTZON et al., 1991) and the use of FLAIR MRI which is more sensitive to low gadolinium concentrations (Bozzao et al., 2003; Dechambre et al., 2000), CSF enhancement may become more commonly recognized than before.

3.2.1. Gadolinium enhancement with contrast-enhanced perfusion imaging

Kao et al. (2003) were the first to demonstrate gadolinium entering the CSF in the lateral ventricles through the choroid plexus after an intravenous GBCA bolus injection in healthy participants (Kao et al., 2003). Dynamic-susceptibility-contrast (DSC) MR perfusion imaging immediately after intravenous administration of a GBCA was used to measure the spatiotemporal contrast distribution (Rempp et al., 1994). Independent component analysis (Hyvärinen and Oja, 2000) with thresholding and Bayesian estimation was then used to provide a segmentation of brain tissues. Post-contrast imaging was conducted for 70 s, and the results showed gadolinium enhancement in the lateral ventricles delayed by several seconds compared to enhancement in the arteries and white and grey matter, which the authors interpreted as GBCA passage through the BCSFB. Later, Wu et al. (2007) obtained similar results using DSC MR perfusion imaging immediately after intravenous administration of a GBCA in healthy participants and post-contrast imaging conducted for 70 s, combined with multivariate Gaussians (Bishop, 1995) and the expectation maximization algorithm (Dempster et al., 1977; Wu et al., 2007).

Bouzerar et al. (2013) investigated choroid plexus functionality using DSC MR perfusion imaging after the first-passage of an intravenous GBCA bolus injection in patients with small cerebral lesions (Bouzerar et al., 2013). These authors found no relation between age and cerebral blood volume or cerebral blood flow in the choroid plexus (Bouzerar et al., 2013). However, choroidal capillary permeability significantly decreased with age, which is in accordance with CSF secretion significantly decreasing with age (May et al., 1990). Decrease in capillary permeability could be due to a decrease in the exchange area or thickening of the capillary basement membrane (Serot et al., 2001a).

Table 2
Overview of included human studies.

Study	Sample	Age in years	MRI technique	Contrast agent type and dosage	Injection method	Imaging delay time after contrast injection	Indicator of BCSFB permeability
Hsu et al. (2005)	Child with craniosynosthosis and hydrocephalus Man with focal seizure	5 and 52	Pre- and post-contrast T1-weighted	0.1 mmol/kg magnevist	Intravenous	Immediately after	Presence of diffuse CSF enhancement compared to pre-contrast
Kao et al. (2003)	5 healthy participants	Age range: 18–47	DSC MR perfusion	20 ml 0.5 mmol/mL Gd-DTPA-BMA	Intravenous	Immediately after	Hemodynamic parameter calculation of the lateral ventricles
Wu et al. (2007)	5 healthy participants	Age range: 18–47	DSC MR perfusion	20 ml 0.5 mmol/mL Gd-DTPA-BMA	Intravenous	Immediately after	Hemodynamic parameter calculation of the lateral ventricles
Bouzerar et al. (2013)	15 patients with small cerebral lesions	Age range: 21–68	DSC MR perfusion	0.1 ml/kg Gd-DOTA	Intravenous	Immediately after	Hemodynamic parameter calculation of the choroid plexus
Kim et al. (2020)	51 MS patients 32 NMOSD patients 28 healthy controls	Median age MS: 39 Median age NMSOD: 50 Median age healthy controls: 48	Post-contrast T1-weighted	Gadolinium-based	Intravenous	Immediately after	Ratio between intensity in the brightest part of the choroid plexus and adjacent white matter
Eide et al. (2019)	8 healthy controls 9 iNPH patients	Mean age healthy controls: 38 Mean age iNPH patients: 68	Pre- and post-contrast T1-weighted	0.5 ml 1.0 mmol/mL gadobutrol	Intrathecal	1.5–2, 2–4, 4–6, 6–9, 24 and 48 h	Larger intensity increase in the choroid plexus and lateral ventricles after a longer delay time means impaired clearance function at the BCSFB
Deike-Hofman et al. (2019)	7 patients with cerebral metastases 33 neurologically healthy patients	Mean age cerebral metastases patients: 66 Mean age neurologically healthy patients: 64	Pre- and post-contrast hT2w-FLAIR	0.1 ml/kg gadovist	Intravenous	3 and 24 h	Intensity increase in the choroid plexus and CSF cavities
Ohashi et al. (2020)	26 patients with suspected endolymphatic hydrops	Age range: 21–80 years	3D-real-IR	0.1 mmol/kg Gd-HP-DO3A	Intravenous	5 min and 4 h	Intensity increase in the lateral ventricle, Sylvian fissure and cisterns
Sudarshana et al. (2019)	8 healthy participants	Age range: 18–70 years	Pre- and post-contrast MEMRI	5 μmol/kg Mangafodipir trisodium	Intravenous	0–2, 4 and/or 6 h 1, 2, 3, 4, 5, 6 and/or 7 days 1, 2 and/or 3 months	Intensity increase in the choroid plexus

Abbreviations: DSC = dynamic-susceptibility-contrast; Gd-DTPA-BMA = gadodiamide (gadolinium- diethylenetriamine pentaacetic acid bismethylamide); Gd-DOTA = gadoterate meglumine (gadolinium- dodecane tetraacetic acid); SWI = susceptibility-weighted imaging; FLAIR = fluid-attenuated inversion recovery; Gd-DTPA = gadopentetate dimeglumine (gadolinium- diethylenetriamine pentaacetic acid); MS = multiple sclerosis; NMSOD = neuromyelitis optica spectrum disorder; iNPH = idiopathic normal pressure hydrocephalus; hT2w-FLAIR = heavily T2-weighted FLAIR; 3D-real-IR = three-dimensional-real inversion recovery; Gd-HP-DO3A = gadoteridol (gadolinium-1,4,7- tris (carboxymethyl)-10-(2' hydroxypropyl)-1,4,7-10-tetraazacyclododecane); MEMRI = manganese-enhanced MRI.

3.2.2. Gadolinium enhancement with post-contrast T1-weighted and post-contrast FLAIR imaging

Kim et al. (2020) aimed to investigate changes in choroid plexus permeability in multiple sclerosis (MS) and neuromyelitis optica spectrum disorder (NMOSD) (Kim et al., 2020), as these are immune-mediated CNS disorders and the choroid plexus is known to regulate the immune response (Baecher-Allan et al., 2018). Using T1-weighted imaging immediately after intravenous administration of a GBCA, the ratio between signal intensity in the brightest part of the choroid plexus and the adjacent white matter was calculated. This enhancement ratio was indeed higher for patients with MS and NMSOD relative to healthy controls (Kim et al., 2020). Due to the absence of a BBB, the choroid plexus always shows enhancement after contrast administration, but the authors state that processes increasing permeability in the choroid plexus capillaries and the BCSFB potentiate contrast extravasation and increase gadolinium enhancement.

3.2.3. Longer delay times

As contrast agent distribution over the CSF takes time, delayed gadolinium imaging, beyond the usual time of approximately 10 min after contrast administration, could be implemented to obtain a better understanding of the CSF pathways (Naganawa et al., 2014).

The discovery of the glymphatic system has led to a renewed interest in waste clearance from the brain (Eide et al., 2019; Verheggen et al., 2018). Eide et al. (2019) used pre- and post-contrast T1-weighted MRI with a longer delay after intrathecal administration of a GBCA to investigate clearance through the choroid plexus (Eide et al., 2019). While previous studies focused on GBCA entering the CSF (Jost et al., 2017; Hsu and Chen, 2005; Kao et al., 2003), this study focused on GBCA being removed from the CSF. Using pre- and post-contrast T1-weighted MRI, they demonstrated increased signal intensity in the choroid plexus and lateral ventricles at 6–9 hours and 24 h after intrathecal contrast administration. This was said to indicate that the choroid plexus is involved in clearance from the brain. The enhancement was stronger in idiopathic normal pressure hydrocephalus (iNPH) patients, indicating a slower clearance rate.

3.2.4. New techniques

So far, studies have primarily been performed in patients with neurologic diseases, for instance in conditions such as acute stroke (Renú et al., 2017), MS (Kim et al., 2020), or iNPH (Eide and Ringstad, 2019). More sensitive imaging sequences are needed to investigate subtle changes in BCSFB permeability in healthy individuals.

Deike-Hofman et al. (2019) used hT2w-FLAIR, sensitive to subtle

gadolinium enhancement in the CSF, before, and 3 and 24 h after intravenous administration of a GBCA (Deike-Hofmann et al., 2019). GBCA distribution through the CNS was visualized and tracked in neurologically healthy patients (Fig. 2) and patients with known BBB disruption.

Increase in signal intensity in the post-contrast images compared to the pre-contrast images was calculated. The results demonstrated that the choroid plexus is an important point of entry of GBCAs into the CSF, which implies that the notion of intravenous substances infiltrating the CNS only through BBB disruption needs to be revised. Prolonged presence of GBCAs in the CSF cavities and increased and prolonged enhancement of the perivascular spaces (Freeze et al., 2017; Naganawa et al., 2017) might be an indicator of glymphatic dysfunction. This GBCA enhancement being associated with the presence of white matter hyperintensities could imply that imaging features of the glymphatic system could have diagnostic value. The study follows the pathway of intact gadolinium complexes through the brain, which might become a diagnostic tool for glymphatic system assessment, and differs from permanent depositions of released gadolinium in the brain (Rasschaert et al., 2020).

GBCAs can end up in the CSF (Naganawa et al., 2017) or brain parenchyma (Kanda et al., 2014), even in healthy individuals. In a recent study, Ohashi et al. (2020) speculated that the pathway by which GBCAs end up in the CNS can be determined by measuring gadolinium enhancement in various CSF spaces (lateral ventricles, Sylvian fissure and cisterns) and in the vitreous, as enhancement is expected to be stronger at locations close to the leakage site (Ohashi et al., 2020). The choroid plexus surrounds the lateral ventricles, so if the choroid plexus is the main leakage site, the highest GBCA concentration would be expected in the lateral ventricles. The authors included patients with suspected endolymphatic hydrops, in which excessive endolymph fluid builds up in the inner ear, as this condition was already being evaluated using three-dimensional-real inversion recovery (3D-real IR) imaging. In 3D-real IR imaging, phase-sensitive reconstruction is used instead of magnitude reconstruction. With phase-sensitive reconstruction, signal intensity is also dependent on the polarity of the magnetization, with more negative values displayed darker, allowing visualization of positive and negative magnetization separately (Park et al., 1986). Magnitude reconstruction only considers the magnitude of the magnetization, with values around the zero-point being darker. As CSF has a negative magnetization, low gadolinium concentrations can actually bring the value closer to the zero-point and paradoxically decrease signal intensity when using magnitude reconstruction. Phase-sensitive construction prevents this paradoxical signal loss and is better at distinguishing fluid compartments and tissue types (Ohashi et al., 2020; Naganawa et al., 2019a). 3D-real IR was used before, and 5 min and 4 h after intravenous GBCA administration. After 4 h, significant increase in signal intensity compared to pre-contrast was found in all CSF locations. However, the signal increase was higher in the cerebral cisternal CSF than in the lateral ventricular CSF. The authors speculate that the choroid plexus could just be one part of the CSF circulation, instead of the main pathway of leakage into the CSF (Ohashi et al., 2020; Orešković et al., 2017), which contradicts previous studies (Jost et al., 2017; Deike--Hofmann et al., 2019).

3.2.5. *Other contrast agents*

The aforementioned contrast agent manganese has been gaining attention, but in humans, manganese can potentially be neurotoxic (Tuschl et al., 2013). Mangafodipir is a chelate that undergoes dephosphorylation and transmetallation after intravenous injection, and slowly releases manganese ions (Runge, 2000). Magnafodipir has been approved and can be used for manganese-enhanced MRI (MEMRI) in humans.

Sudarshana et al. (2019) used MEMRI in healthy participants with T1-weighted MRI before and at various time points after intravenous administration of mangafodipir. (Sudarshana et al., 2019) The authors demonstrated that structures surrounded by the BBB did not show any manganese enhancement when comparing post-contrast with pre-contrast images, while the choroid plexus did (Sudarshana et al., 2019; Wang et al., 1997). Signal intensity in the choroid plexus increased within the first hour after contrast administration, and reached maximum intensity after a time interval of 11−40 min. Signal intensity was returned to pre-contrast level around 5–7 days after administration. However, as opposed to the findings in rats, the CSF and surroundings of the brain parenchyma did not show any manganese enhancement, but the manganese dose derived from mangafodipir was also much lower than the dose derived from manganese chloride delivered to rats. Manganese in the blood can be transported over the BBB as well as the BCSFB, but as the blood levels increase, the manganese ions preferably accumulate for transport into the CSF at the choroid plexus (Yokel, 2009; Schmitt et al., 2011). Within the choroid plexus, the distribution of manganese is similar to that of gadolinium.

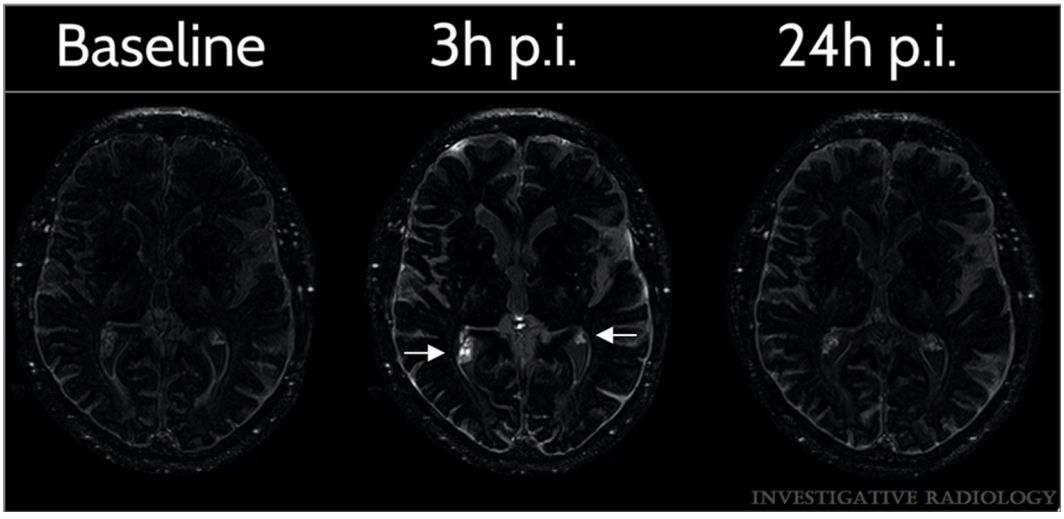

Fig. 2. Gadolinium enhancement in the choroid plexus using heavily T2-weighted fluid-attenuated inversion recovery. Images obtained from a 64-year-old male patient with bronchial carcinoma, without neurological disorder and with normal renal function. Gadolinium enhancement after intravenous administration of a single dose of gadolinium-based contrast agent is detected with heavily T2-weighted fluid-attenuated inversion recovery, with first pre-contrast baseline, then 3 h post injection (3 h p.i.) and lastly 24 h post injection (24 h p.i.). The choroid plexus demonstrates strong contrast enhancement after 3 h (arrows) compared to baseline. Figure adapted from Deike-Hofman et al. (2019) (118) with permission.

Manganese enhancement is, however, thought to especially visualize the cellular components of tissue, and not the intravascular spaces, which may facilitate delineation of tissue borders (Fig. 3) (Sudarshana et al., 2019).

4. Discussion

The role of BBB disruption in pathological disorders such as AD and in processes such as aging and neurodegeneration has been gaining great interest over the last decade (van de Haar et al., 2016; Farrall and Wardlaw, 2009; Freeze et al., 2020). As the BBB is important for exchanging vital biomolecules, blocking pathogens and clearing waste products from the brain tissue, BBB disruption can lead to disruption of homeostasis in the CNS and disturb the chemical balance required for neuronal functioning (Zlokovic, 2008). However, the composition of the CSF is also important for the balance in the CNS, and BCSFB function is essential in maintaining this composition (Segal, 2000). The BCSFB has already been demonstrated to deteriorate during aging, and this deterioration is exacerbated in AD (Balusu et al., 2016; Serot et al., 2003). Moreover, the choroid plexus epithelial cells of the BCSFB are essential for T-lymphocyte signaling, which is involved in neuroprotection and hippocampus-dependent cognitive functions (Ziv et al., 2006; Moalem et al., 1999). Aging has been associated with dysregulation of T-lymphocyte signaling in the choroid plexus, which can have consequences for CNS integrity and cognitive functioning (Baruch et al., 2013). The role of BCSFB disruption in brain pathology and neurodegeneration should be further investigated, starting with a greater focus on imaging techniques to measure BCSFB permeability.

4.1. Developments in contrast-enhanced MRI for blood-cerebrospinal fluid barrier permeability assessment

Post-contrast T1-weighted and FLAIR imaging with intravenous administration of a GBCA have been used to detect gadolinium enhancement in the ventricles, and it was concluded that gadolinium can enter the CSF through the BCSFB. Most of these studies, both in animals and humans, were conducted under pathological conditions, such as genetic deficits (Yang et al., 2019), meningitis (Ichikawa and Itoh, 2011), acute stroke (Renú et al., 2017) or MS (Kim et al., 2020). In these conditions, signal intensity in the ventricles increased after contrast administration, which was thought to be indicative of BCSFB disruption.

The presence of gadolinium in the CSF has been confirmed in a study that used mass spectrometry of CSF samples obtained with lumbar puncture from patients who had previously undergone gadolinium-enhanced MRI (Nehra et al., 2018). CSF samples were obtained at random time points after contrast-enhanced imaging, and gadolinium in the CSF could be detected already 1.1 h after administration, and could still be detected up to 24 days after administration. Moreover, patients were said to have an intact BBB with a CSF total protein concentration lower than 35 mg/dl, and even in these patients, gadolinium could be detected more than 10 days after administration. According to the authors, this immediate and persistent gadolinium enhancement in the CSF, even with an intact BBB, suggests that the choroid plexus, arachnoid granulations and glymphatic system all play a role in CSF and CNS gadolinium distribution.

In vivo imaging studies are also investigating longer imaging delay times after contrast administration. Gadolinium enhancement was demonstrated to peak several hours after contrast administration (Naganawa et al., 2020a). To visualize the CSF pathways in the brain, imaging should be conducted over an extended time period. Although this will not give additional information on the initial blood-to-CSF transfer, investigating whether contrast accumulates near the choroid plexus after several hours can provide information on the involvement of the BCSFB in clearing compounds from the CSF.

Another promising new development is the use of hT2w-FLAIR imaging, which is more sensitive to subtle gadolinium leakage into the CSF compared to regular FLAIR scans (with shorter echo times), and has already been successfully applied in both rats and humans (Jost et al., 2016; Deike-Hofmann et al., 2019). 3D-real IR imaging, which takes into account the negative magnetization of the CSF, is another promising technique (Ohashi et al., 2020). Both of these techniques can be used to detect subtle contrast enhancement in the CSF of healthy subjects.

Studies are also considering the use of other contrast agents than gadolinium. Manganese ions, for example, appear hyperintense on post-contrast T1-weighted images and have a longer enhancement window after administration compared to GBCAs (Wesolowski and Kaiser, 2016). Manganese-enhanced (ME) MRI has demonstrated that manganese accumulates in the choroid plexus in both rats and humans (Aoki et al., 2004; Sudarshana et al., 2019). While in the rat brain, manganese enhancement could also be detected in the CSF and periventricular structures (Aoki et al., 2004), this has not been found in humans yet, where lower concentrations were used (Sudarshana et al., 2019). Animal studies are also being conducted using VSOPs as contrast agent, as these particles can be used for cell labelling through phagocytosis and highlight barrier disruptions (Millward et al., 2013). Another recent development is the combination of MRI with optical imaging. In mice studies, eu-VSOPs have been administered, which have superparamagnetic as well as fluorescence properties, and can be used not only for contrast-enhanced MRI, but also for fluorescence microscopy and immunostaining with the advantage of being able to confirm the in vivo findings (Millward et al., 2019).

It is important to note that, while this review exclusively focused on contrast-enhanced MRI, there could be contrast-free approaches to assess BCSFB integrity. A recent, important development is for instance the use of non-invasive, tracer-free BCSFB arterial spin labelling (ASL) (Evans et al., 2020). An ASL MRI sequence is used to label blood water in the feeding arteries and capture how this water crosses the BCSFB into the ventricular CSF. An ultra-long echo time is used, so that the signal from the blood and brain tissue will almost fully decay, while signal

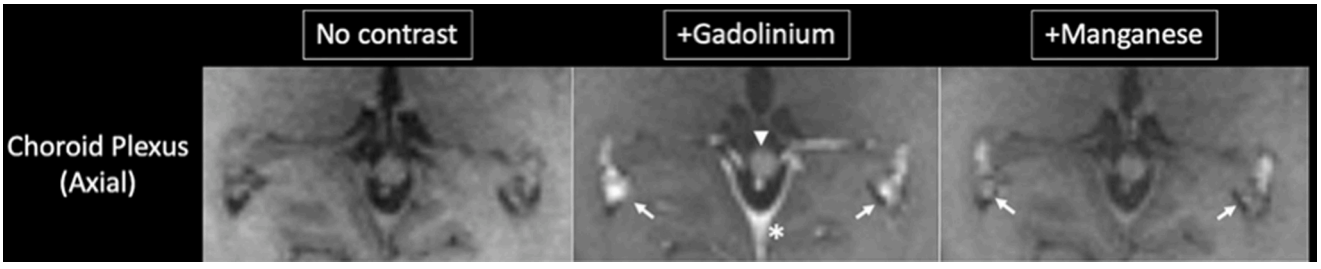

Fig. 3. Gadolinium enhancement compared to manganese enhancement. Images obtained approximately 20 min after gadolinium administration and 1 h after mangafodipir administration. After intravenous administration of a gadolinium-based contrast agent, enhancement can be seen in the choroid plexus (arrows), posterior falx cerebri (asterisk), and pineal gland (arrowhead). After intravenous administration of mangafodipir, however, the choroid glomus enhances in a heterogeneous manner. Note the enhancement of the vasculature (posterior falx cerebri (asterisk) where the posterior meningeal artery can be found) with gadolinium, but not with manganese. Figure adapted from Sudarshana et al. (2019) (129) with permission.

from the CSF is preserved due to the long T2 relaxation time of the CSF. Also, low spatial resolution is used, so that small signals can be detected (i.e., discerned from noise) due to the relatively large voxel size, as partial volume effects from the surrounding brain tissue cannot influence the signal due to the ultra-long echo time. Applying this technique, a significantly decreased BCSFB-mediated water delivery in aged mice relative to adult mice was found, and the authors state that these findings suggest that BCSFB function might play an important role in the initial stages of neurodegeneration and might meet the urgent need for early biomarkers of neurodegeneration. BCSFB ASL still needs to be investigated in the human brain, and it would be interesting if future studies could compare this promising method to the contrast-enhanced MRI methods described in this review.

4.2. Limitations

While the present review provides a comprehensive overview of the available studies that assessed BCSFB permeability with contrast-enhanced MRI, there are several limitations that complicate the interpretation of the reported findings. Firstly, the presence of contrast material in the CSF does not necessarily have to imply BCSFB breakdown, as there are alternative routes through which contrast agents can reach the CSF (Naganawa et al., 2020a). For example, BBB breakdown could be another route, although contrast agents passing from the blood into the brain parenchyma and then being cleared into the CSF is generally thought to take longer (Gaohua et al., 2016). Other points through which contrast agents can enter the CSF, even in healthy conditions, are the anterior eye segment (Naganawa et al., 2011), the peripheral part of the cranial nerves (Naganawa et al., 2014) and the CVOs (Verheggen et al., 2020b). Also, several recent studies have demonstrated that intravenously administered contrast agent can leak from the cortical veins into the surrounding CSF (Naganawa et al., 2019b; Naganawa et al., 2020b, 2020c). The contrast agent can permeate the sparse pial sheath of the venous wall of the cortical veins into the subarachnoid space. With longer delay after contrast administration, the contrast agent can also be distributed over the CSF by the glymphatic system (Iliff et al., 2013). Recently, the existence of meningeal lymphatic vessels along the superior sagittal sinus was discovered (Aspelund et al., 2015; Wu et al., 2021). These meningeal lymphatic vessels are thought to drain CSF into the cervical lymph nodes, and are for instance involved in the clearance of Aβ (Da Mesquita et al., 2018; Naganawa and Taoka, 2020). CSF enhancement could thus be attributed to a mix of BBB disruption, BCSFB disruption and glymphatic dysfunction (Naganawa et al., 2020a).

Secondly, CSF contrast enhancement is not only related to contrast agent entering the CSF, but probably also to the CSF secretion rate and turnover. Especially at longer delay times after contrast administration, any leaked contrast will remain in the CSF longer when the CSF clearance rate is lower (Pul et al., 2015).

Thirdly, the extent of CSF enhancement due to BCSFB disruption is probably dependent on the contrast agent dosage, the specific MR sequence parameters used, and the assessment method of CSF enhancement (i.e., visual inspection, contrast enhancement ratio, hemodynamic parameter calculation, etc.). For this reason, it is very difficult to directly compare the findings of the individual studies in this review.

Finally, the detection of contrast extravasation at the level of the choroid plexus does not necessarily have to indicate BCSFB disruption, as it is part of normal choroid plexus and BCSFB functioning to secrete filtrated blood plasma into the CSF (Balusu et al., 2016). Also, several studies conducted in healthy animals and humans have demonstrated post-contrast changes at the level of the choroid plexus and ventricles (Jost et al., 2017; Deike-Hofmann et al., 2019; Ohashi et al., 2020). When using contrast-enhanced MRI to assess BCSFB functioning, it remains unclear to what extent the findings can be attributed to normal functioning, or BCSFB disruption. Future studies should therefore include appropriate control samples for comparison.

4.3. Conclusion

The BCSFB is involved in the composition of the CSF and thus the maintenance of homeostasis in the CNS, but how BCSFB disruption relates to age-related neurodegeneration is underassessed. This review focused on how contrast enhancement on MRI has been used to assess BCSFB permeability. Post-contrast gadolinium enhancement in the ventricles has revealed BCSFB disruption and new techniques are being developed, for instance imaging sequences that are highly sensitive to the CSF (hT2w-FLAIR, 3D-real IR) or the use of contrast agents other than gadolinium-based compounds (manganese, VSOPs). By further promoting these sorts of developments, we believe much progress can still be made in the assessment of BCSFB integrity.

Funding

This work was supported by the Nederlandse Organisatie voor Wetenschappelijk Onderzoek (NWO) [grant number 406-15-031].

Declaration of Competing Interest

None.

References

Abbott, N.J., Pizzo, M.E., Preston, J.E., Janigro, D., Thorne, R.G., 2018. The role of brain barriers in fluid movement in the CNS: is there a 'glymphatic' system? Acta Neuropathol. 135 (3), 387–407.
Agarwal, N., Contarino, C., Toro, E.F., 2019. Neurofluids: a holistic approach to their physiology, interactive dynamics and clinical implications for neurological diseases. Veins Lymphat. 8 (3).
Aoki, I., Y-JL, Wu, Silva, A.C., Lynch, R.M., Koretsky, A.P., 2004. In vivo detection of neuroarchitecture in the rodent brain using manganese-enhanced MRI. Neuroimage 22 (3), 1046–1059.
Aspelund, A., Antila, S., Proulx, S.T., Karlsen, T.V., Karaman, S., Detmar, M., et al., 2015. A dural lymphatic vascular system that drains brain interstitial fluid and macromolecules. J. Exp. Med. 212 (7), 991–999.
Baecher-Allan, C., Kaskow, B.J., Weiner, H.L., 2018. Multiple sclerosis: mechanisms and immunotherapy. Neuron 97 (4), 742–768.
Balusu, S., Brkic, M., Libert, C., Vandenbroucke, R.E., 2016. The choroid plexus-cerebrospinal fluid interface in Alzheimer's disease: more than just a barrier. Neural Regen. Res. 11 (4), 534.
Baruch, K., Ron-Harel, N., Gal, H., Deczkowska, A., Shifrut, E., Ndifon, W., et al., 2013. CNS-specific immunity at the choroid plexus shifts toward destructive Th2 inflammation in brain aging. Proc. Natl. Acad. Sci. 110 (6), 2264–2269.
Baruch, K., Kertser, A., Porat, Z., Schwartz, M., 2015. Cerebral nitric oxide represses choroid plexus NF κB-dependent gateway activity for leukocyte trafficking. EMBO J. 34 (13), 1816–1828.
Bateman, G.A., Brown, K.M., 2012. The measurement of CSF flow through the aqueduct in normal and hydrocephalic children: from where does it come, to where does it go? Childs Nerv. Syst. 28 (1), 55–63.
Batra, A., Latour, L.L., Ruetzler, C.A., Hallenbeck, J.M., Spatz, M., Warach, S., et al., 2010. Increased plasma and tissue MMP levels are associated with BCSFB and BBB disruption evident on post-contrast FLAIR after experimental stroke. J. Cereb. Blood Flow Metab. 30 (6), 1188–1199.
Bergen, A.A., Kaing, S., Jacoline, B., Gorgels, T.G., Janssen, S.F., 2015. Gene expression and functional annotation of human choroid plexus epithelium failure in Alzheimer's disease. BMC Genomics 16 (1), 956.
Bishop, C.M., 1995. Neural Networks for Pattern Recognition. Oxford university press.
Borlongan, C., Skinner, S., Geaney, M., Vasconcellos, A., Elliott, R., Emerich, D., 2004. CNS grafts of rat choroid plexus protect against cerebral ischemia in adult rats. Neuroreport 15 (10), 1543–1547.
Bouzerar, R., Chaarani, B., Gondry-Jouet, C., Zmudka, J., Balédent, O., 2013. Measurement of choroid plexus perfusion using dynamic susceptibility MR imaging: capillary permeability and age-related changes. Neuroradiology 55 (12), 1447–1454.
Bozzao, A., Floris, R., Fasoli, F., Fantozzi, L., Colonnese, C., Simonetti, G., 2003. Cerebrospinal fluid changes after intravenous injection of gadolinium chelate: assessment by FLAIR MR imaging. Eur. Radiol. 13 (3), 592–597.
Brinker, T., Stopa, E., Morrison, J., Klinge, P., 2014. A new look at cerebrospinal fluid circulation. Fluids Barriers CNS 11, 10.
Chalbot, S., Zetterberg, H., Blennow, K., Fladby, T., Andreasen, N., Grundke-Iqbal, I., et al., 2011. Blood-cerebrospinal fluid barrier permeability in Alzheimer's disease. J. Alzheimer's Dis. 25 (3), 505–515.
Chen, R.L., Athauda, S.B., Kassem, N.A., Zhang, Y., Segal, M.B., Preston, J.E., 2005. Decrease of transthyretin synthesis at the blood–cerebrospinal fluid barrier of old sheep. J. Gerontol. Ser. A: Biol. Sci. Med. Sci. 60 (7), 852–858.

Chen, R., Kassem, N., Redzic, Z., Chen, C., Segal, M., Preston, J., 2009. Age-related changes in choroid plexus and blood–cerebrospinal fluid barrier function in the sheep. Exp. Gerontol. 44 (4), 289–296.
Chen, G.-f, Xu, T.-h, Yan, Y., Zhou, Y.-r, Jiang, Y., Melcher, K., et al., 2017. Amyloid beta: structure, biology and structure-based therapeutic development. Acta Pharmacologica Sinica 38 (9), 1205.
Christensen, J., Wright, D.K., Yamakawa, G.R., Shultz, S.R., Mychasiuk, R., 2020. Repetitive mild traumatic brain injury alters glymphatic clearance rates in limbic structures of adolescent female rats. Sci. Rep. 10 (1), 1–9.
Crossgrove, J.S., Li, G.J., Zheng, W., 2005. The choroid plexus removes β-amyloid from brain cerebrospinal fluid. Exp. Biol. Med. 230 (10), 771–776.
Da Mesquita, S., Fu, Z., Kipnis, J., 2018. The meningeal lymphatic system: a new player in neurophysiology. Neuron 100 (2), 375–388.
Davson, H., Segal, M.B., 1996. Physiology of the CSF and Blood-brain Barriers. CRC press.
De Leon, M., DeSanti, S., Zinkowski, R., Mehta, P., Pratico, D., Segal, S., et al., 2004. MRI and CSF studies in the early diagnosis of Alzheimer's disease. J. Internal Med. 256 (3), 205–223.
Dechambre, S., Duprez, T., Grandin, C., Lecouvet, F., Peeters, A., Cosnard, G., 2000. High signal in cerebrospinal fluid mimicking subarachnoid haemorrhage on FLAIR following acute stroke and intravenous contrast medium. Neuroradiology 42 (8), 608–611.
Deike-Hofmann, K., Reuter, J., Haase, R., Paech, D., Gnirs, R., Bickelhaupt, S., et al., 2019. Glymphatic pathway of gadolinium-based contrast agents through the brain: overlooked and misinterpreted. Investig. Radiol. 54 (4), 229–237.
Dempster, A.P., Laird, N.M., Rubin, D.B., 1977. Maximum likelihood from incomplete data via the EM algorithm. J. R. Stat. Soc. Ser. B (Methodological). 39 (1), 1–22.
DiNuzzo, M., Nedergaard, M., 2017. Brain energetics during the sleep–wake cycle. Curr. Opin. Neurobiol. 47, 65–72.
Eide, P.K., Ringstad, G., 2019. Delayed clearance of cerebrospinal fluid tracer from entorhinal cortex in idiopathic normal pressure hydrocephalus: a glymphatic magnetic resonance imaging study. J. Cereb. Blood Flow Metab. 39 (7), 1355–1368.
Eide, P.K., Valnes, L.M., Pripp, A.H., Mardal, K.-A., Ringstad, G., 2019. Delayed clearance of cerebrospinal fluid tracer from choroid plexus in idiopathic normal pressure hydrocephalus. J. Cereb. Blood Flow Metab. 0271678X19874790.
Emerich, D.F., Skinner, S.J., Borlongan, C.V., Vasconcellos, A.V., Thanos, C.G., 2005. The choroid plexus in the rise, fall and repair of the brain. Bioessays 27 (3), 262–274.
Engelhardt, B., Ransohoff, R.M., 2005. The ins and outs of T-lymphocyte trafficking to the CNS: anatomical sites and molecular mechanisms. Trends Immunol. 26 (9), 485–495.
Erdő, F., Denes, L., de Lange, E., 2017. Age-associated physiological and pathological changes at the blood–brain barrier: a review. J. Cereb. Blood Flow Metab. 37 (1), 4–24.
Evans, P., Sokolska, M., Alves, A., Harrison, I., Ohene, Y., Nahavandi, P., et al., 2020. Non-invasive MRI of blood–Cerebrospinal fluid barrier function. Nat. Commun. 11 (1), 1–11.
Farrall, A.J., Wardlaw, J.M., 2009. Blood–brain barrier: ageing and microvascular disease–systematic review and meta-analysis. Neurobiol. Aging 30 (3), 337–352.
Feldner, A., Adam, M.G., Tetzlaff, F., Moll, I., Komljenovic, D., Sahm, F., et al., 2017. Loss of Mpdz impairs ependymal cell integrity leading to perinatal-onset hydrocephalus in mice. EMBO Mol. Med. 9 (7), 890–905.
Fishman, R.A., 2002. The cerebrospinal fluid production rate is reduced in dementia of the Alzheimer's type. Neurology 58 (12), 1866.
Freeze, W., Schnerr, R., Palm, W., Jansen, J., Jacobs, H., Hoff, E., et al., 2017. Pericortical enhancement on delayed postgadolinium fluid-attenuated inversion recovery images in normal aging, mild cognitive impairment, and Alzheimer disease. Am. J. Neuroradiol. 38 (9), 1742–1747.
Freeze, W., Ter Weele, D., Palm, W., van Hooren, R., Hoff, E., Jansen, J., et al., 2019. Optimal detection of subtle gadolinium leakage in CSF with heavily T2-weighted fluid-attenuated inversion recovery imaging. Am. J. Neuroradiol. 40 (9), 1481–1483.
Freeze, W.M., Jacobs, H.I., de Jong, J.J., Verheggen, I.C., Gronenschild, E.H., Palm, W. M., et al., 2020. White matter hyperintensities mediate the association between blood-brain barrier leakage and information processing speed. Neurobiol. Aging 85, 113–122.
Gaberel, T., Gakuba, C., Goulay, R., De Lizarrondo, S.M., Hanouz, J.-L., Emery, E., et al., 2014. Impaired glymphatic perfusion after strokes revealed by contrast-enhanced MRI. Stroke 114, 006617.
Gaohua, L., Neuhoff, S., Johnson, T.N., Rostami-Hodjegan, A., Jamei, M., 2016. Development of a permeability-limited model of the human brain and cerebrospinal fluid (CSF) to integrate known physiological and biological knowledge: estimating time varying CSF drug concentrations and their variability using in vitro data. Drug Metab. Pharmacokinet. 31 (3), 224–233.
Ghersi-Egea, J.F., Strazielle, N., 2001. Brain drug delivery, drug metabolism, and multidrug resistance at the choroid plexus. Microsc. Res. Tech. 52 (1), 83–88.
Gideon, P., Thomsen, C., Ståhlberg, F., Henriksen, O., 1994. Cerebrospinal fluid production and dynamics in normal aging: a MRI phase-mapping study. Acta Neurologica Scandinavica 89 (5), 362–366.
Goldim, M.P., Danielski, L.G., Rodrigues, J.F., Joaquim, L., Garbossa, L., de Oliveira Junior, A.N., et al., 2019. Oxidative stress in the choroid plexus contributes to blood–cerebrospinal fluid barrier disruption during sepsis development. Microvascular Res. 123, 19–24.
Hladky, S.B., Barrand, M.A., 2014. Mechanisms of fluid movement into, through and out of the brain: evaluation of the evidence. Fluids Barriers CNS 11 (1), 1.
Hsu, H.L., Chen, C.J., 2005. Extensive cerebrospinal fluid enhancement following gadolinium chelate administration: possible pathogenesis. Acta Radiol. 46 (5), 523–527.
Hyvärinen, A., Oja, E., 2000. Independent component analysis: algorithms and applications. Neural Networks 13 (4–5), 411–430.
Ichikawa, H., Itoh, K., 2011. Blood–arachnoid barrier disruption in experimental rat meningitis detected using gadolinium-enhancement ratio imaging. Brain Res. 1390, 142–149.
Ichikawa, H., Ishikawa, M., Fukunaga, M., Ishikawa, K., Ishiyama, H., 2010. Quantitative evaluation of blood–cerebrospinal fluid barrier permeability in the rat with experimental meningitis using magnetic resonance imaging. Brain Res. 1321, 125–132.
Ikeda, T., Furukawa, Y., Mashimoto, S., Takahashi, K., Yamada, M., 1990. Vitamin B12 levels in serum and cerebrospinal fluid of people with Alzheimer's disease. Acta Psychiatrica Scandinavica. 82 (4), 327–329.
Iliff, J.J., Wang, M., Liao, Y., Plogg, B.A., Peng, W., Gundersen, G.A., et al., 2012. A paravascular pathway facilitates CSF flow through the brain parenchyma and the clearance of interstitial solutes, including amyloid β. Sci. Transl. Med. 4 (147), 147ra11-ra11.
Iliff, J.J., Lee, H., Yu, M., Feng, T., Logan, J., Nedergaard, M., et al., 2013. Brain-wide pathway for waste clearance captured by contrast-enhanced MRI. J. Clin. Investing. 123 (3), 1299–1309.
Johanson, C.E., 2017. Chapter 11 - choroid Plexus–Cerebrospinal fluid transport dynamics: support of brain health and a role in neurotherapeutics. In: Conn, P.M. (Ed.), Conn's Translational Neuroscience. Academic Press, San Diego, pp. 233–261.
Jost, G., Lenhard, D.C., Sieber, M.A., Lohrke, J., Frenzel, T., Pietsch, H., 2016. Signal increase on unenhanced T1-weighted images in the rat brain after repeated, extended doses of gadolinium-based contrast agents: comparison of linear and macrocyclic agents. Investig. Radiol. 51 (2), 83.
Jost, G., Frenzel, T., Lohrke, J., Lenhard, D.C., Naganawa, S., Pietsch, H., 2017. Penetration and distribution of gadolinium-based contrast agents into the cerebrospinal fluid in healthy rats: a potential pathway of entry into the brain tissue. Eur. Radiol. 27 (7), 2877–2885.
Kanda, T., Ishii, K., Kawaguchi, H., Kitajima, K., Takenaka, D., 2014. High signal intensity in the dentate nucleus and globus pallidus on unenhanced T1-weighted MR images: relationship with increasing cumulative dose of a gadolinium-based contrast material. Radiology 270 (3), 834–841.
Kao, Y.H., Guo, W.Y., Wu, Y.T., Liu, K.C., Chai, W.Y., Lin, C.Y., et al., 2003. Hemodynamic segmentation of MR brain perfusion images using independent component analysis, thresholding, and Bayesian estimation. Magn. Reson. Med. 49 (5), 885–894.
Kesslak, J.P., So, V., Choi, J., Cotman, C.W., Gomez-Pinilla, F., 1998. Learning upregulates brain-derived neurotrophic factor messenger ribonucleic acid: a mechanism to facilitate encoding and circuit maintenance? Behav. Neurosci. 112 (4), 1012.
Khasawneh, A.H., Garling, R.J., Harris, C.A., 2018. Cerebrospinal fluid circulation: what do we know and how do we know it? Brain Circ. 4 (1), 14.
Kim, H., Lim, Y.-M., Kim, G., Lee, E.-J., Lee, E.-J., Kim, H.W., et al., 2020. Choroid plexus changes on magnetic resonance imaging in multiple sclerosis and neuromyelitis optica spectrum disorder. J. Neurological Sci., 116904
KNUTZON, R.K., POIRIER, V.C., Gerscovich, E.O., BROCK, J.M., BUONOCORE, M., 1991. The effect of intravenous gadolinium on the magnetic resonance appearance of cerebrospinal fluid. Investig. Radiol. 26 (7), 671–673.
Kobayashi, Y., Hauptmann, R., Kratz, H., Ebert, M., Wagner, S., Taupitz, M., 2017. Europium doping of superparamagnetic iron oxide nanoparticles enables their detection by fluorescence microscopy and for quantitative analytics. Technol. Health Care 25 (3), 457–470.
Kress, B.T., Iliff, J.J., Xia, M., Wang, M., Wei, H.S., Zeppenfeld, D., et al., 2014. Impairment of paravascular clearance pathways in the aging brain. Ann. Neurol. 76 (6), 845–861.
Li, M.D., Kane, J.K., Matta, S.G., Blaner, W.S., Sharp, B.M., 2000. Nicotine enhances the biosynthesis and secretion of transthyretin from the choroid plexus in rats: implications for β-amyloid formation. J. Neurosci. 20 (4), 1318–1323.
Liddelow, S.A., 2015. Development of the choroid plexus and blood-CSF barrier. Front. Neurosci. 9 (32).
May, C., Kaye, J., Atack, J.R., Schapiro, M., Friedland, R., Rapoport, S., 1990. Cerebrospinal fluid production is reduced in healthy aging. Neurology 40 (3 Part 1), 500-.
Mesquita, S.D., Ferreira, A.C., Sousa, J.C., Santos, N.C., Correia-Neves, M., Sousa, N., et al., 2012. Modulation of iron metabolism in aging and in Alzheimer's disease: relevance of the choroid plexus. Front. Cell. Neurosci. 6, 25.
Millward, J.M., Schnorr, J., Taupitz, M., Wagner, S., Wuerfel, J.T., Infante-Duarte, C., 2013. Iron Oxide Magnetic Nanoparticles Highlight Early Involvement of the Choroid Plexus in Central Nervous System Inflammation.
Millward, J.M., Ariza de Schellenberger, A., Berndt, D., Hanke-Vela, L., Schellenberger, E., Waiczies, S., et al., 2019. Application of europium-doped very small Iron oxide nanoparticles to visualize neuroinflammation with MRI and fluorescence microscopy. Neuroscience 403, 136–144.
Milner, L.C., Shirley, R.L., Kozell, L.B., Walter, N.A., Kruse, L.C., Komiyama, N.H., et al., 2015. Novel MPDZ/MUPP1 transgenic and knockdown models confirm Mpdz's role in ethanol withdrawal and support its role in voluntary ethanol consumption. Addict. Biol. 20 (1), 143–147.
Moalem, G., Leibowitz–Amit, R., Yoles, E., Mor, F., Cohen, I.R., Schwartz, M., 1999. Autoimmune T cells protect neurons from secondary degeneration after central nervous system axotomy. Nat. Med. 5 (1), 49–55.
Montagne, A., Zhao, Z., Zlokovic, B.V., 2017. Alzheimer's disease: a matter of blood–brain barrier dysfunction? J. Exp. Med. 214 (11), 3151–3169.

Montaner, J., Alvarez-Sabín, J., Molina, C., Anglés, A., Abilleira, S., Arenillas, J., et al., 2001. Matrix metalloproteinase expression after human cardioembolic stroke: temporal profile and relation to neurological impairment. Stroke 32 (8), 1759–1766.
Naganawa, S., Taoka, T., 2020. The glymphatic system: a review of the challenges in visualizing its structure and function with MR imaging. Magn. Resonan. Med. Sci. rev. 2020-0122.
Naganawa, S., Kawai, H., Sone, M., Nakashima, T., 2010. Increased sensitivity to low concentration gadolinium contrast by optimized heavily T2-weighted 3D-FLAIR to visualize endolymphatic space. Magn. Resonan. Med. Sci. 9 (2), 73–80.
Naganawa, S., Yamazaki, M., Kawai, H., Sone, M., Nakashima, T., 2011. Contrast enhancement of the anterior eye segment and subarachnoid space: detection in the normal state by heavily T2-weighted 3D FLAIR. Magn. Resonan. Med. Sci. 10 (3), 193–199.
Naganawa, S., Suzuki, K., Yamazaki, M., Sakurai, Y., 2014. Serial scans in healthy volunteers following intravenous administration of gadoteridol: time course of contrast enhancement in various cranial fluid spaces. Magn. Resonan. Med. Sci. 13 (1), 7–13.
Naganawa, S., Nakane, T., Kawai, H., Taoka, T., 2017. Gd-based contrast enhancement of the perivascular spaces in the basal ganglia. Magn. Resonan. Med. Sci. 16 (1), 61–65.
Naganawa, S., Kawai, H., Taoka, T., Sone, M., 2019a. Improved 3D-real inversion recovery: a robust imaging technique for endolymphatic hydrops after intravenous administration of gadolinium. Magn. Resonan. Med. Sci. 18 (1), 105.
Naganawa, S., Nakane, T., Kawai, H., Taoka, T., 2019b. Age dependence of gadolinium leakage from the cortical veins into the cerebrospinal fluid assessed with whole brain 3D-real inversion recovery MR imaging. Magn. Resonan. Med. Sci. 18 (2), 163–169.
Naganawa, S., Ito, R., Kato, Y., Kawai, H., Taoka, T., Yoshida, T., et al., 2020a. Intracranial distribution of intravenously administered gadolinium-based contrast agent over a period of 24 hours: evaluation with 3D-real IR imaging and MR fingerprinting. Magn. Resonan. Med. Sci mp. 2020-0030.
Naganawa, S., Ito, R., Nakamichi, R., Kawamura, M., Kawai, H., Taoka, T., et al., 2020b. Relationship between parasagittal perivenous cysts and leakage of gadolinium-based contrast agents into the subarachnoid space around the cortical veins after intravenous administration. Magn. Resonan. Med. Sci mp. 2020-0062.
Naganawa, S., Nakane, T., Kawai, H., Taoka, T., Kawaguchi, H., Maruyama, K., et al., 2020c. Detection of IV-gadolinium leakage from the cortical veins into the CSF using MR fingerprinting. Magn. Resonan. Med. Sci. 19 (2), 141.
Natah, S.S., Srinivasan, S., Pittman, Q., Zhao, Z., Dunn, J.F., 2009. Effects of acute hypoxia and hyperthermia on the permeability of the blood-brain barrier in adult rats. J. Appl. Physiol. 107 (4), 1348–1356.
Nathoo, N., Jalal, H., Natah, S.S., Zhang, Q., Wu, Y., Dunn, J.F., 2016. Hypoxia and inflammation-induced disruptions of the blood-brain and blood-cerebrospinal fluid barriers assessed using a novel t 1-Based MRI method. Brain Edema XVI, 23–28. Springer.
Nehra, A.K., McDonald, R.J., Bluhm, A.M., Gunderson, T.M., Murray, D.L., Jannetto, P.J., et al., 2018. Accumulation of gadolinium in human cerebrospinal fluid after gadobutrol-enhanced MR imaging: a prospective observational cohort study. Radiology 288 (2), 416–423.
Nixon, P.F., Jordan, L., Zimitat, C., Rose, S.E., Zelaya, F., 2008. Choroid plexus dysfunction: the initial event in the pathogenesis of Wernicke's encephalopathy and ethanol intoxication. Alcohol. Clin. Exp. Res. 32 (8), 1513–1523.
Ohashi, T., Naganawa, S., Iwata, S., Kuno, K., 2020. Distribution of gadolinium-based contrast agent after leaking into the cerebrospinal fluid: comparison between the cerebral cisterns and the lateral ventricles. Magn. Resonan. Med. Sci mp. 2020-0016.
Okamura, T., Ishibashi, N., Zurakowski, D., Jonas, R.A., 2010. Cardiopulmonary bypass increases permeability of the blood-cerebrospinal fluid barrier. Ann. Thorac. Surg. 89 (1), 187–194.
Orešković, D., Klarica, M., 2010. The formation of cerebrospinal fluid: nearly a hundred years of interpretations and misinterpretations. Brain Res. Rev. 64 (2), 241–262.
Orešković, D., Klarica, M., 2014. A new look at cerebrospinal fluid movement. Fluids Barriers CNS 11 (1), 16.
Orešković, D., Radoš, M., Klarica, M., 2017. Role of choroid plexus in cerebrospinal fluid hydrodynamics. Neuroscience 354, 69–87.
Ott, B.R., Jones, R.N., Daiello, L.A., de la Monte, S.M., Stopa, E.G., Johanson, C.E., et al., 2018. Blood-cerebrospinal fluid barrier gradients in mild cognitive impairment and alzheimer's disease: relationship to inflammatory cytokines and chemokines. Front. Aging Neurosci. 10 (245).
Park, H., Cho, M., Cho, Z., 1986. Real-value representation in inversion-recovery NMR imaging by use of a phase-correction method. Magn. Resonan. Med. 3 (1), 15–23.
Pfister, H.-W., Fontana, A., Täuber, M.G., Tomasz, A., Scheld, W.M., 1994. Mechanisms of brain injury in bacterial meningitis: workshop summary. Clin. Infect. Dis. 19 (3), 463–479.
Preston, J., 1999. Age-related reduction in rat choroid plexus chloride efflux and CSF secretion rate. editor Soc. Neurosci.
Pul, R., Yildiz, Ö, Morbiducci, F., Skripuletz, T., Schwenkenbecher, P., Stangel, M., et al., 2015. CSF levels of angiopoietin-2 do not differ between patients with CSF fluid leakage syndrome and controls. Dis. Markers 2015.
Raja, R., Rosenberg, G.A., Caprihan, A., 2018. MRI measurements of Blood-Brain Barrier function in dementia: a review of recent studies. Neuropharmacology 134, 259–271.
Rasschaert, M., Weller, R.O., Schroeder, J.A., Brochhausen, C., Idée, J.M., 2020. Retention of gadolinium in brain parenchyma: pathways for speciation, access, and distribution. A critical review. J. Magn. Resonan. Imaging.
Rempp, K.A., Brix, G., Wenz, F., Becker, C.R., Gückel, F., Lorenz, W.J., 1994. Quantification of regional cerebral blood flow and volume with dynamic susceptibility contrast-enhanced MR imaging. Radiology 193 (3), 637–641.
Renú, A., Laredo, C., Lopez-Rueda, A., Llull, L., Tudela, R., San-Roman, L., et al., 2017. Vessel Wall enhancement and blood–cerebrospinal fluid barrier disruption after mechanical thrombectomy in acute ischemic stroke. Stroke 48 (3), 651–657.
Roberts, T.P., Mikulis, D., 2007. Neuro MR: principles. J. Magn. Resonan. Imaging 26 (4), 823–837.
Runge, V.M., 2000. Safety of approved MR contrast media for intravenous injection. J. Magn. Resonan. Imaging. 12 (2), 205–213.
Saito, S., Aoki, I., Sawada, K., Sun, X.-Z., Chuang, K.-H., Kershaw, J., et al., 2011. Quantitative and noninvasive assessment of prenatal X-ray-induced CNS abnormalities using magnetic resonance imaging. Radiat. Res. 175 (1), 1–9.
Schmitt, C., Strazielle, N., Richaud, P., Bouron, A., Ghersi-Egea, J.F., 2011. Active transport at the blood-CSF barrier contributes to manganese influx into the brain. J. Neurochem. 117 (4), 747–756.
Schubert, J.J., Veronese, M., Marchitelli, L., Bodini, B., Tonietto, M., Stankoff, B., et al., 2019. Dynamic 11C-PiB PET shows cerebrospinal fluid flow alterations in Alzheimer disease and multiple sclerosis. J. Nuclear Med. 60 (10), 1452–1460.
Segal, M.B., 2000. The choroid plexuses and the barriers between the blood and the cerebrospinal fluid. Cell. Mol. Neurobiol. 20 (2), 183–196.
Selhub, J., Troen, A., Rosenberg, I.H., 2010. B vitamins and the aging brain. Nutr. Rev. 68 (suppl_2). S112-S8.
Serot, J., Christmann, D., Dubost, T., Couturier, M., 1997. Cerebrospinal fluid transthyretin: aging and late onset Alzheimer's disease. J. Neurology Neurosurg. Psychiatry 63 (4), 506–508.
Serot, J.-M., Béné, M.-C., Foliguet, B., Faure, G.C., 2000. Morphological alterations of the choroid plexus in late-onset Alzheimer's disease. Acta Neuropathologica 99 (2), 105–108.
Serot, J.M., Foliguet, B., Béné, M.C., Faure, G.C., 2001a. Choroid plexus and ageing in rats: a morphometric and ultrastructural study. Eur. J. Neurosci. 14 (5), 794–798.
Serot, J., Christmann, D., Dubost, T., Bene, M., Faure, G., 2001b. CSF-folate levels are decreased in late-onset AD patients. J. Neural Trans. 108 (1), 93–99.
Serot, J.-M., Béné, M.-C., Faure, G.C., 2003. Choroid plexus, aging of the brain, and Alzheimer's disease. Front Biosci. 8, s515–21 (suppl).
Shearer, G.M., 1997. Th1/Th2 changes in aging. Mech Ageing Dev. 94 (1-3), 1–5.
Silverberg, G., Heit, G., Huhn, S., Jaffe, R., Chang, S., Bronte–Stewart, H., et al., 2001. The cerebrospinal fluid production rate is reduced in dementia of the Alzheimer's type. Neurology 57 (10), 1763–1766.
Silverberg, G.D., Mayo, M., Saul, T., Rubenstein, E., McGuire, D., 2003. Alzheimer's disease, normal-pressure hydrocephalus, and senescent changes in CSF circulatory physiology: a hypothesis. Lancet Neurol. 2 (8), 506–511.
Smith, A.J., Verkman, A.S., 2019. CrossTalk opposing view: going against the flow: interstitial solute transport in brain is diffusive and aquaporin-4 independent. J. Physiol. 597 (17), 4421–4424.
Spector, R., Robert Snodgrass, S., Johanson, C.E., 2015a. A balanced view of the cerebrospinal fluid composition and functions: focus on adult humans. Exp. Neurol. 273, 57–68.
Spector, R., Keep, R.F., Robert Snodgrass, S., Smith, Q.R., Johanson, C.E., 2015b. A balanced view of choroid plexus structure and function: focus on adult humans. Exp. Neurol. 267, 78–86.
Starr, J.M., Farrall, A.J., Armitage, P., McGurn, B., Wardlaw, J., 2009. Blood–brain barrier permeability in Alzheimer's disease: a case–control MRI study. Psychiatry Res. Neuroimaging 171 (3), 232–241.
Stevenson, N.J., Addley, M.R., Ryan, E.J., Boyd, C.R., Carroll, H.P., Paunovic, V., et al., 2009. CCL11 blocks IL-4 and GM-CSF signaling in hematopoietic cells and hinders dendritic cell differentiation via suppressor of cytokine signaling expression. J. Leukocyte Biol. 85 (2), 289–297.
Stroh, A., Zimmer, C., Werner, N., Gertz, K., Weir, K., Kronenberg, G., et al., 2006. Tracking of systemically administered mononuclear cells in the ischemic brain by high-field magnetic resonance imaging. Neuroimage 33 (3), 886–897.
Sudarshana, D.M., Nair, G., Dwyer, J.T., Dewey, B., Steele, S.U., Suto, D.J., et al., 2019. Manganese-enhanced MRI of the brain in healthy volunteers. Am J. Neuroradiol. 40 (8), 1309–1316.
Sundaram, S., Hughes, R.L., Peterson, E., Müller-Oehring, E.M., Bronte-Stewart, H.M., Poston, K.L., et al., 2019. Establishing a framework for neuropathological correlates and glymphatic system functioning in Parkinson's disease. Neurosci. Biobehav. Rev. 103, 305–315.
Tang, Y.P., Haslam, S.Z., Conrad, S.E., Sisk, C.L., 2004. Estrogen increases brain expression of the mRNA encoding transthyretin, an amyloid β scavenger protein. J. Alzheimer's Dis. 6 (4), 413–420.
Tanna, N.K., Kohn, M.I., Horwich, D.N., Jolles, P.R., Zimmerman, R.A., Alves, W.M., et al., 1991. Analysis of brain and cerebrospinal fluid volumes with MR imaging: impact on PET data correction for atrophy. Part II. Aging and Alzheimer dementia. Radiology 178 (1), 123–130.
Taoka, T., Naganawa, S., 2020. Imaging for central nervous system (CNS) interstitial fluidopathy: disorders with impaired interstitial fluid dynamics. Japanese J. Radiol.
Tuschl, K., Mills, P.B., Clayton, P.T., 2013. Manganese and the brain. Int. Rev. Neurobiol. 110, 277–312. Elsevier.
van de Haar, H.J., Burgmans, S., Hofman, P.A., Verhey, F.R., Jansen, J.F., Backes, W.H., 2014. Blood-brain barrier impairment in dementia: current and future in vivo assessments. Neurosci. Biobehav. Rev.
van de Haar, H.J., Burgmans, S., Jansen, J.F., van Osch, M.J., van Buchem, M.A., Muller, M., et al., 2016. Blood-brain barrier leakage in patients with early Alzheimer disease. Radiology 281 (2), 527–535.
Vargas, T., Ugalde, C., Spuch, C., Antequera, D., Morán, M.J., Martín, M.A., et al., 2010. Aβ accumulation in choroid plexus is associated with mitochondrial-induced apoptosis. Neurobiol. Aging 31 (9), 1569–1581.

Verheggen, I., Van Boxtel, M., Verhey, F., Jansen, J., Backes, W., 2018. Interaction between blood-brain barrier and glymphatic system in solute clearance. Neurosci. Biobehav. Rev. 90, 26–33.
Verheggen, I.C., de Jong, J.J., van Boxtel, M.P., Gronenschild, E.H., Palm, W.M., Postma, A.A., et al., 2020a. Increase in blood–brain barrier leakage in healthy, older adults. GeroScience 1–11.
Verheggen, I.C., de Jong, J.J., van Boxtel, M.P., Postma, A.A., Verhey, F.R., Jansen, J.F., et al., 2020b. Permeability of the windows of the brain: feasibility of dynamic contrast-enhanced MRI of the circumventricular organs. Fluids Barriers CNS 17 (1), 1–13.
Vitek, M.P., Bhattacharya, K., Glendening, J.M., Stopa, E., Vlassara, H., Bucala, R., et al., 1994. Advanced glycation end products contribute to amyloidosis in Alzheimer disease. Proc. Natl. Acad. Sci. 91 (11), 4766–4770.
Wang, C., Gordon, P., Hustvedt, S., Grant, D., Sterud, A.T., Martinsen, I., et al., 1997. MR imaging properties and pharmacokinetics of MnDPDP in healthy volunteers. Acta Radiologica 38 (5), 665–676.
Wen, G.Y., Wisniewski, H.M., Kascsak, R.J., 1999. Biondi ring tangles in the choroid plexus of Alzheimer's disease and normal aging brains: a quantitative study. Brain Res. 832 (1–2), 40–46.
Wesolowski, J.R., Kaiser, A., 2016. Alternatives to GBCA: are we there yet? Top. Magn. Resonance Imaging 25 (4), 171–175.
Wilson, M., Preston, J., Thomas, S., Segal, M., 1999. Altered cerebrospinal fluid secretion rate and 125I-labelled-amyloid transport in the aged sheep isolated perfused choroid plexus. J. Physiol.(London) 515, 7P.
Wolburg, H., Paulus, W., 2010. Choroid plexus: biology and pathology. Acta Neuropathologica 119 (1), 75–88.
Wu, Y.T., Chou, Y.C., Guo, W.Y., Yeh, T.C., Hsieh, J.C., 2007. Classification of spatiotemporal hemodynamics from brain perfusion MR images using expectation-maximization estimation with finite mixture of multivariate gaussian distributions. Magn. Reson. Med. 57 (1), 181–191.
Wu, C.-H., Lirng, J.-F., Ling, Y.-H., Wang, Y.-F., Wu, C.-H., Fuh, J.-L., et al., 2021. Noninvasive characterization of human glymphatics and meningeal lymphatics in an in vivo model of blood–Brain barrier leakage. Ann. Neurol. n/a(n/a).
Wuerfel, J., Tysiak, E., Prozorovski, T., Smyth, M., Mueller, S., Schnorr, J., et al., 2007. Mouse model mimics multiple sclerosis in the clinico-radiological paradox. Eur. J. Neurosci. 26 (1), 190–198.
Yang, J., Simonneau, C., Kilker, R., Oakley, L., Byrne, M.D., Nichtova, Z., et al., 2019. Murine MPDZ-linked hydrocephalus is caused by hyperpermeability of the choroid plexus. EMBO Mol. Med. 11 (1), e9540.
Yokel, R.A., 2009. Manganese flux across the blood–brain barrier. Neuromol. Med. 11 (4), 297–310.
Ziv, Y., Ron, N., Butovsky, O., Landa, G., Sudai, E., Greenberg, N., et al., 2006. Immune cells contribute to the maintenance of neurogenesis and spatial learning abilities in adulthood. Nat. Neurosci. 9 (2), 268–275.
Zlokovic, B.V., 2008. The blood-brain barrier in health and chronic neurodegenerative disorders. Neuron 57 (2), 178–201.